

Experimental Investigation on Heat Transfer and Film Cooling of High Loaded Transonic Turbine Vanes and Blades

Ryouma NOGAMI¹, Kunihiro SHIMIZU¹,
Kenichiro TAKEISHI² and Tsuyoshi KITAMURA²

¹ Mitsubishi Heavy Industries, LTD.
Nagoya Guidance & Propulsion Systems Works
1200, Higashi-tanaka, Komaki, Aichi 485-8561, JAPAN
Phone: +81-568-79-0324, FAX: +81-568-79-3025, E-mail: Ryoma_Nogami@mhi.co.jp
² Mitsubishi Heavy Industries, LTD.
Takasago Research & Development Center

ABSTRACT

The demand for the reduction of aero-engines weight and improvement of fuel consumption remains high for the purpose of reducing CO₂. Therefore the turbine blade cooling air of the aero-engines reduces relatively and the turbine specification achieves a high pressure ratio with fewer number of stage i.e. highly-loaded. Advanced cooling technologies applied for high loaded turbines have been earnestly investigated. High performance cooling methods and accurate estimation of heat transfer around airfoils are requested to improve turbine vanes and blades' life.

In this study, high speed cascade tests with typical high loaded transonic turbine vane and blade have been conducted to investigate the flow field, the heat transfer and the film cooling effectiveness around blade surface.

NOMENCLATURE

A	Area
C	Concentration of a tracer
M	Mach number or mass flux ratio
T	Temperature
U	Velocity
p	Pressure
q	Net heat transfer flux
α	Heat transfer coefficient
η_f	Film cooling effectiveness
κ	Ratio of specific heats
ρ	Density

Subscripts

a	Air
aw	Adiabatic wall
bs	Blade surface
ch	Chamber
ex	Exit
x	local point
2	Secondary fluid
∞	Mainstream

INTRODUCTION

ESPR (research and development of Environmentally

compatible propulsion system for next-generation SuPeRsonic transport) program was initiated in 1999 as the successor of HYPR (super/HYper-sonic transport Propulsion system Research and development) program by NEDO (New Energy and industrial technology Development Organization) under METI (Ministry of Economy, Trade and Industry) budget support in order to develop necessary technologies for the next-generation SST engine. The program overview was reported by TOKUMASU et al. (2002).

In ESPR program, CO₂, NOx and noise reduction technologies are especially focused as environmentally compatible technologies, which are critical to realize next-generation SST. 25% reduction has been chosen as engine CO₂ reduction target. The target should be realized by reduction of engine weight and improvement of fuel consumption under development of advanced material application technology and advanced secondary air cooling technology. The heat transfer and film cooling effectiveness about high loaded and high pressure ratio turbines are confirmed experimentally in this paper.

EXPERIMENTAL MEASUREMENT ON HEAT TRANSFER FOR A HIGH LOADED AND HIGH PRESSURE TURBINE BLADE

High speed cascade tests with typical high loaded transonic turbine blade have been conducted to acquire the heat transfer coefficient around the blade surface.

Test Blade

Test cascade is the mean section of a typical high pressure turbine blade. The specifications are the inlet flow angle 51.3 degree, the exit Mach number of 1.12 and the turning angle 105 degree. Figure 1 shows the test blade. The exit Mach number can be calculated from the following definition.

$$M_{ex} = \sqrt{\frac{2}{\kappa - 1} \left\{ \left(\frac{p_{ch}}{p_{ex}} \right)^{(\kappa-1)/\kappa} - 1 \right\}} \quad (1)$$

Test rig

The measurements were conducted in a linear turbine cascade facility with seven test blades as shown in figure 2. For heat transfer

test, the measurement blade was located at the center of linear cascade. The local heat transfer coefficient is derived from the measured heat flux of an electrically heated nickel foil divided by the difference of the main stream temperature and blade surface temperature, which was measured by embedded thermocouples in the blade surface. Figure 3 shows the heat transfer measurement blade. The accuracy of the heat transfer coefficient is ± 10 percent. The measurement blade was equipped with 50 thermocouples. For blade surface static pressure test, the measurement blades equipped with 14 pressure taps on suction side and 8 pressure taps on pressure side were located at the side of center blade. Figure 4 shows the position of measurement blades. The test rig has measurement windows for flow visualization by color schlieren method.

Experimental results and discussion

Static pressure at the blade surface and flow visualization

The measurement of the static pressure at blade surface and flow visualization were conducted in order to confirm the location and strength of the shock wave. Figure 5 shows the measured results and the analytical prediction about the static pressure at the exit Mach number of 1.12. The static pressure distribution around blade surface was predicted in good accuracy. Figure 6 shows the color schlieren photography. Figure 7 shows the schematic of color schlieren photography. In figure 5, the static pressure on the suction surface rises around the non-dimensional surface length of 0.8 because of shock wave. This location is in good agreement with that of shock boundary layer interaction caught sharply by color schlieren photography in figure 6.

Heat transfer coefficient at the blade surface

The measurement of the local heat transfer coefficient at the blade surface was conducted. The local heat transfer coefficient α can be calculated from the measured local net heat transfer flux q , the local blade surface temperature T_{bs} at the position of the thin nickel foil and the local air temperature T_a .

$$\alpha = \frac{q}{A(T_{bs} - T_a)} \quad (2)$$

The local net heat flux q is derived from the electric power generated by nickel foil heater. Figure 8 shows measured heat transfer coefficient distribution on the blade surface at the exit Mach number of 1.12. Although shock boundary interaction clearly generates at the suction surface of the blade in the color schlieren photography shown in figure 6, the local blade surface heat transfer coefficient shown in figure 8 does not show strong increase generated by shock wave. The shock wave has a weak influence on the heat transfer on suction surface up to the exit Mach number of 1.1 because the strong shock wave with the separated and reattached flow does not generate.

HIGH LOADED TRANSONIC TURBINE VANE CASCADE TEST

High speed cascade tests with the high loaded transonic turbine vane have been conducted to investigate the film cooling effectiveness.

Test Blade

The turbine model airfoils were used for the two-dimensional high speed cascade tests. The airfoils were a first stage vane mean section for a typical aero-gas-turbine high pressure turbine. The specifications are the pressure ratio 2.31, the inlet flow angle 0 degree, the exit Mach number of 1.16 and the exit flow angle 71.8 degree. The exit Mach number can be calculated from Eq.(1). The vane is equipped with single row of film cooling holes on the suction surface. The tests were planned to investigate the film

cooling effectiveness of round hole and shaped hole applied on the suction surface of the test vane. The parameter of geometry is given in table 1. The configuration and dimensions of the film cooling holes are shown in table 2 and figure 9. Figure 10 shows the test vane.

Test rig

The measurement of the film cooling effectiveness was conducted in a linear turbine cascade facility with six test vanes as shown in figure 2. The two center vanes were film cooled vanes (round hole and shaped hole) and the remaining four vanes were solid. Figure 11 shows the position of the measurement vanes. The measurement vane was equipped with 8 suction taps located behind the film cooling holes on suction side, 8 suction taps located between the film cooling holes on suction side and 8 suction taps located on pressure side for film cooling effectiveness measurements.

Measuring method

The film cooling effectiveness was defined by

$$\eta_f = \frac{T_{aw} - T_\infty}{T_2 - T_\infty} \quad (3)$$

Heated or cooled secondary fluid was injected through the film cooling holes and the adiabatic wall temperature T_{aw} was measured. In order to obtain local effectiveness, a large scale model has to be used to decrease thermal conductivity error. It is a very difficult problem to adopt a large size turbine vane made of a low thermal conductivity material for air cascade test rig. So in this study, a mass heat transfer analogy is applied to measure film cooling effectiveness as shown in figure 12. This analogy was used by Takeishi et al. (1992). Local effectiveness η_f is defined as

$$\eta_f = \frac{C_x - C_\infty}{C_2 - C_\infty} \quad (4)$$

The analogy holds if the turbulent Lewis number and the molecular Lewis number are in union (Ito et al., 1978; Pedersen et al., 1977). In this study, helium gas was used for the tracer. Much attention was paid to suction of the film cooling layer on the turbine vane. If the suction speed is too high, mainstream air will mix with the sucked-in air and cause large error. Therefore, examination was carried out by changing the suction speed and a suction speed where the effectiveness is constant was decided upon. The suction speed was kept under 80 to 200 ml/min at each suction tap and the sucked-in air was accumulated in the air bag. Later, the concentration of helium in the sucked-in air in the bag was analyzed by using gas chromatography. The concentration of helium was 1000 ppm, 0 ppm at the film cooling hole exit and mainstream, respectively. Therefore $C_\infty \doteq 0$ and eq.(4) can be described by

$$\eta_f = \frac{C_x}{C_2} \quad (5)$$

The effectiveness was calculated by the data, which were measured several times. The accuracy of the gas chromatography is ± 1 percent.

Experimental results and discussion

Static pressure at the vane surface

The static pressure distribution at the vane surface, which is shown in figure 13, was measured at the exit Mach number of 1.16 by utilizing suction taps on the vane for film cooling effectiveness

measurements. The static pressure on the suction side is local minimum at non-dimensional vane surface length 0.4 and local maximum at 0.5 because of shock boundary layer interaction. The interacting point is located between non-dimensional vane surface length 0.4 and 0.5.

Film cooling effectiveness

The measured averaged film cooling effectiveness on the suction side at the exit Mach number of 1.16 and the blowing ratio 0.8 is shown in figure 14. Blowing ratio M can be calculated from the following definition is defined as

$$M = \frac{\rho_2 U_2}{\rho_\infty U_\infty} \quad (6)$$

The effectiveness data were arranged by using non-dimensional surface length. The effect of the film cooling was confirmed behind film cooling hole. Although shock boundary interaction clearly generates on the suction surface at the exit Mach number of 1.16 as shown in figure 13, the film cooling effectiveness in figure 14 is not affected by shock wave. The shock wave has a weak influence on the film cooling effectiveness on suction surface up to the exit Mach number of 1.1. On the other hand, it was clear that the film cooling effectiveness between film cooling holes in the spanwise direction was approximately 0. Therefore, it was confirmed that the film cooling flow does not diffuse in spanwise direction on the suction surface.

The film cooling effectiveness on the suction surface at the exit Mach number of 1.16 and the blowing ratio 0.8 were shown in figure 15 with the comparison between the round hole and the shaped hole. It is clear from figure 15 that the shaped film cooling holes attain higher film cooling effectiveness than the round film cooling holes.

CONCLUSIONS

High speed cascade tests with typical high loaded transonic turbine vane and blade have been conducted to acquire the heat transfer coefficient and the film cooling effectiveness around blade surface. The following conclusion were obtained through these results:

1. The shock wave has a weak influence on the heat transfer coefficient on suction surface up to the exit Mach number of 1.1.
2. It was confirmed that the film cooling flow does not diffuse in spanwise direction on transonic turbine airfoil suction surface. The test results also show that shaped film cooling holes attain higher film cooling effectiveness than round film cooling holes.

ACKNOWLEDGMENTS

This work was carried out under the entrustment contract with NEDO as a part of the R&D Project on New Industrial Science and Technology Frontiers, Program for Scientific Technology Development for Industries that creates METI.

REFERENCES

Tokumasu, Y. et al., 2001, "Overview of "Research and Development of Environmentally Compatible Propulsion System for Next-Generation Supersonic Transport (ESPR project)", ISABE2001-1179, Bangalore, India
 Takeisghi, K., Aoki, S., Sato T., and Tsukagoshi, K., 1992, "Film Cooling on a Gas Turbine Rotor Blade," *ASME Journal of Turbomachinery*, Vol. 114, pp. 828-834
 Ito, S., Goldstein, R. J., and Eckert, E. R. G., 1978, "Film Cooling on a Gas Turbine Blade," *ASME Journal of Engineering*



Figure 1 Test blade

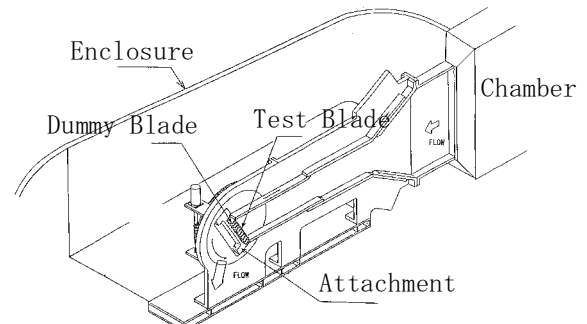


Figure 2 Schematic diagram of test

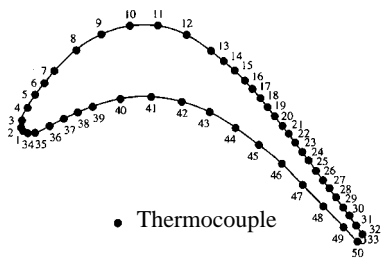


Figure 3 Heat transfer coefficient measurement blade

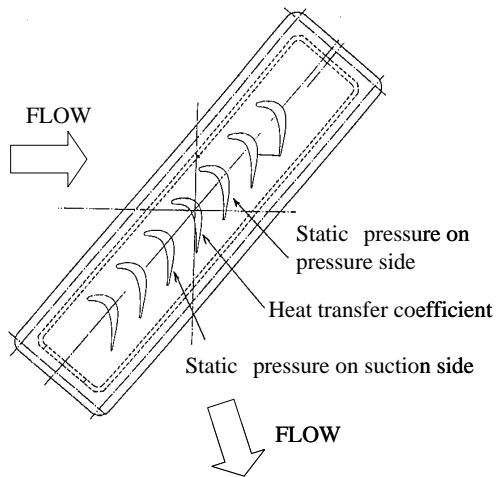


Figure 4 Position of measurement blade

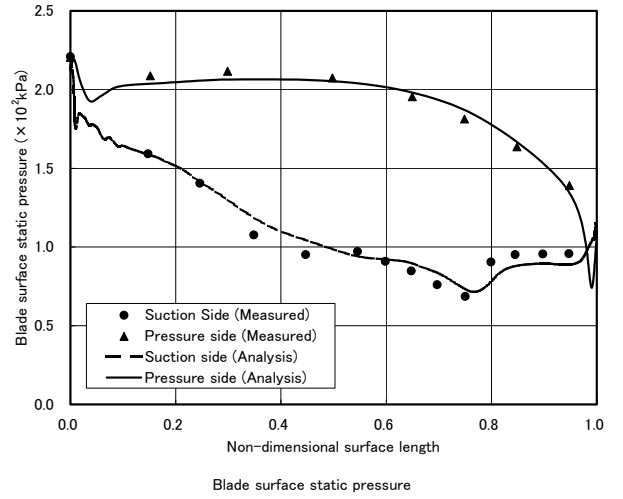
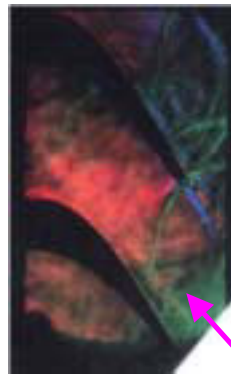


Figure 5 Static pressure distribution on blade surface



Primary shock wave

Figure 6 Color Schlieren photography

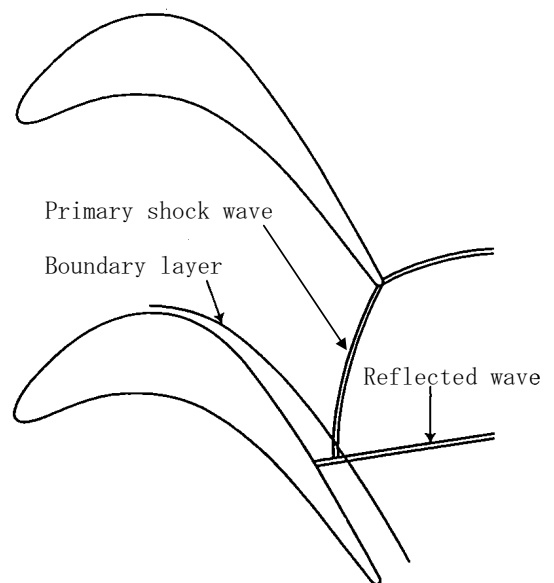


Figure 7 Schematic of color schlieren photography

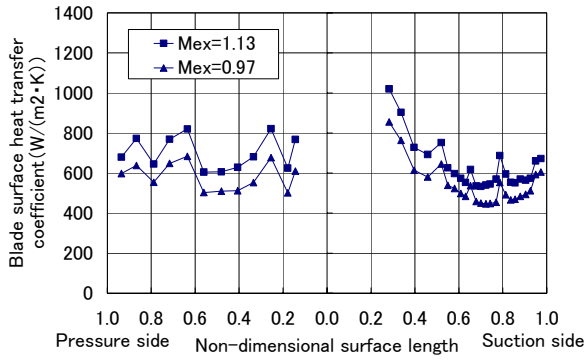
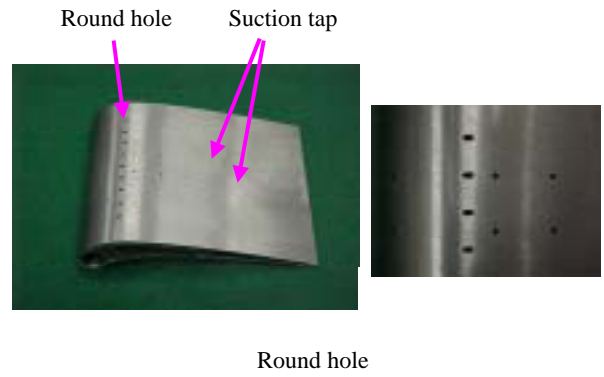


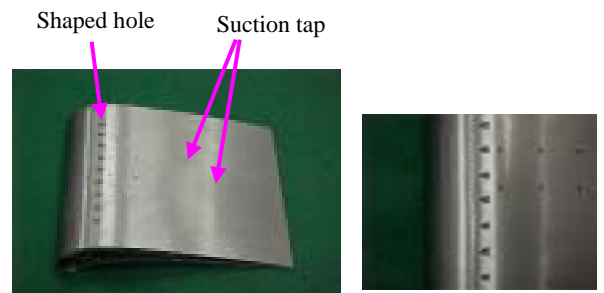
Figure 8 Measured heat transfer coefficient on blade surface



Round hole

Table 1 Vane geometry

Chord length (mm)	105.62
Pitch (mm)	88.31
Throat width (mm)	27.36
Blade height (mm)	90.00
Pitch / Chord length	0.836
Blade height / Chord length	0.852



Shaped hole

Table 2 Film cooling hole dimension

Diameter at suction side (mm)	1.26
Pitch at suction side (mm)	7.70

Figure 10 Test vane



Figure 9 Shaped film cooling hole configuration

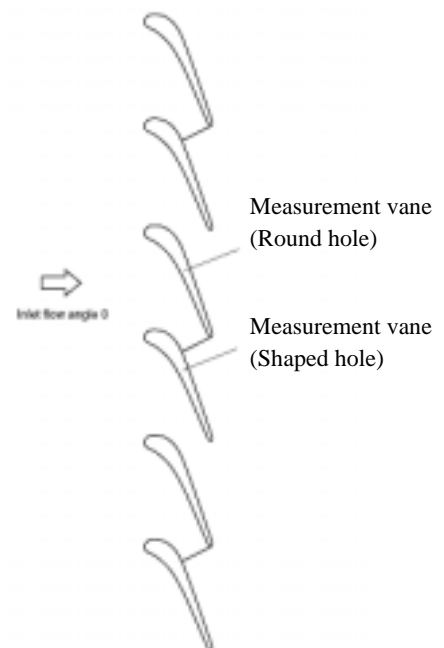


Figure 11 Position of measurement vane

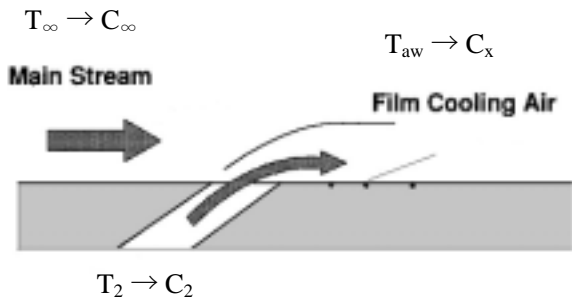


Figure 12 Method of measuring film cooling effectiveness

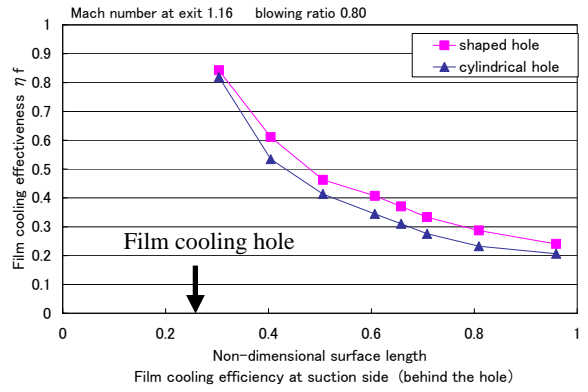


Figure 15 Measured film cooling effectiveness (Round hole and shaped hole)

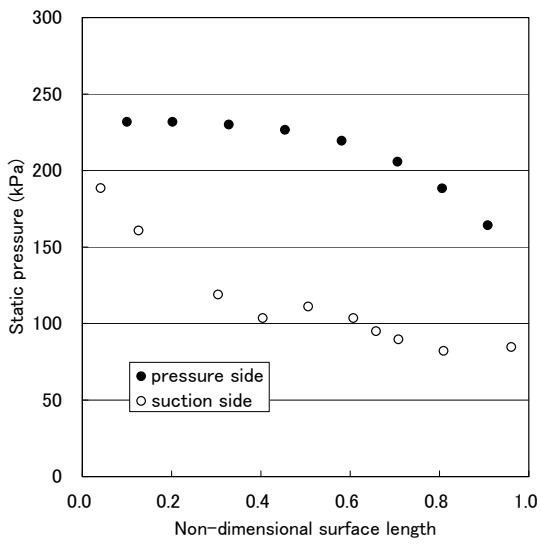


Figure 13 Static pressure distribution of vane surface

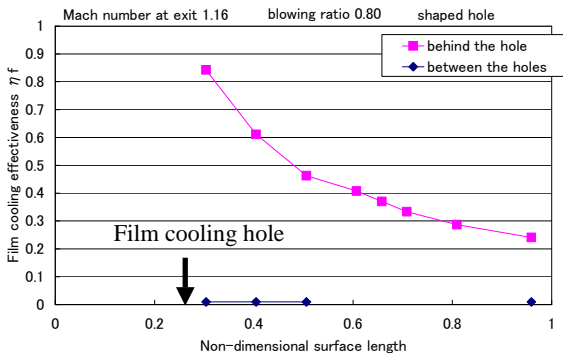


Figure 14 Measured film cooling effectiveness on suction side